Biointerface Research in Applied Chemistry
Open-Access Journal (ISSN: 2069-5837)

Article
Volume 14, Issue 3, 2024, 66
https://doi.org/10.33263/BRIAC143.066

Extraction and Purification of Steroids in the Sea Urchin (*Diadema Setosum* Leske) Gonads with a Three-Component Solvent System

Nasriadi Dali [1,*], Armadi Chairunnas [2], Hilda Ayu Melvi Amalia [3]

[1] Department of Chemistry, Faculty of Mathematics and Natural Sciences, Halu Oleo University, Kendari 93232 - Southeast Sulawesi, Indonesia; nasriadidali@ymail.com (N.D.);
[2] Department of Biology, Faculty of Mathematics and Natural Sciences, University of Nahdlatul 'Ulama Sulawesi Tenggara, Kendari 93563 - Southeast Sulawesi, Indonesia; armadisajami@gmail.com (A.C.);
[3] Study Program of Tadris Biology, Faculty of Tarbiyah and Teacher Training, Institut Agama Islam Negeri (IAIN), Kendari 93563 - Southeast Sulawesi, Indonesia; hildaayumelvi@gmail.com (H.A.M.A.);
* Correspondence: nasriadidali@ymail.com (N.D.);

Scopus Author ID 57190677418
Received: 29.07.2023; Accepted: 20.12.2023; Published: 17.02.2024

Abstract: Research on the extraction and purification of steroids in sea urchins (*Diadema Setosum* Leske) gonads with a three-component solvent system has been successfully carried out. This study aimed to extract and purify steroids in sea urchin gonads using a three-component solvent system (chloroform, methanol, and water) and to determine the type and concentration of steroids in the sea urchin gonads. The sea urchin gonads were extracted with a volume ratio of solvent (chloroform : methanol : water) (1 : 2 : 0.8) before and (2 : 2 : 1.8) after dilution. The liquid extract was in the form of biphase layers, the top and bottom layers were respectively methanol-water extract (glycoside fraction) and chloroform extract (lipid fraction). The chloroform extract was isolated by preparative KKV and TLC methods. The isolate was purified with methanol. Pure isolates were identified for their steroid type by UV-VIS, FTIR, FTNMR 1D, and 2D spectroscopy. Steroid levels in isolates were determined by UV-VIS spectrophotometry. The type of steroid compound obtained is cholesterol (5-kolesten-3β-ol) with a concentration of 5,06%. This indicates that a three-component solvent system can be used to extract steroids from marine natural products.

Keywords: cholesterol, extraction, sea urchin gonads, steroids, three-component solvent systems.

1. Introduction

Steroids are chemicals, often hormones, that our bodies make naturally in small amounts. Steroids help the organs, tissues, and cells in our bodies to do their job in controlling the immune system, regulate the use of food to produce energy (metabolism), maintain the balance of salt and water in the body, regulate blood pressure, reduce allergies and inflammation, and control mood heart and behavior [1-6].

Steroids can also refer to man-made drugs. The two main types are corticosteroids and anabolic-androgenic steroids [7]. Corticosteroids are drugs that quickly fight inflammation in the body. This artificial steroid works like cortisone, a 17-hydroxy-11-dehydrocorticosterone steroid hormone, which is made by the adrenal glands in the body [8]. The hormone cortisone protects the immune system from substances that cause inflammation. Corticosteroid drugs, such as (prednisolone, methylprednisolone, dexamethasone, hydrocortisone), work similarly

to the hormone cortisone in the body [9]. They slow or stop immune system processes that trigger inflammation. Corticosteroids are used to treat a variety of ailments, particularly to relieve symptoms of allergies, irritation, inflammation, eczema, dermatitis, rheumatoid arthritis, asthma, chronic obstructive pulmonary disorder (COPD), lupus and other autoimmune disorders, multiple sclerosis, rashes, and skin conditions like eczema [10-15].

With the properties of steroids that can lower the immune system, they can also be used to prevent rejection reactions of the body against transplanted organs in patients who have recently undergone organ transplants [16]. Steroids are also used for pregnant women who have a risk of premature delivery. Steroids function to mature the fetal lungs, so if you have to be born prematurely, the baby's lungs are strong enough and work well [17]. Steroids are even used in cancer patients. There are a number of reasons steroids have as part of cancer treatment: to prevent nausea and vomiting from chemotherapy, to treat cancer itself, to reduce inflammation, to help prevent allergic reactions, to reduce the body's immune response, to help reduce pain, and to increase the appetite of cancer patients [18-23].

Steroids can also be used as contraceptives. The origin of this birth control pill can be traced back to the wild yam that grows in Mexico. Wild yam are a member of the Dioscoreaceae family, which consists of hundreds of species. However, only four species are relevant for medicinal purposes: *Dioscorea villosa* (found in the United States), *Dioscorea opposita* and *Dioscorea hypoglauca* (native to Asia); and the Mexican yam, *Dioscorea barbasco* [24]. Oral contraceptive pills are a combination of estrogen (estradiol) and progestogen (progestin); when women swallow these pills, they inhibit fertility [25]. The main active chemical agents in wild yam are steroidal saponins, known as diosgenin. It is actually present in wild yam roots as dioscin, a steroidal saponin whose aglycone is diosgenin. *Dioscin glycosides* from the roots of the Mexican wild yam, *Dioscorea*, were the first important plant source of sapogenins for steroid drugs, and these compounds can be chemically converted to the hormone progesterone [26-27].

So many uses of steroids, had become the prima donna of the medical world at the beginning. Its effectiveness in helping cure several kinds of diseases makes its name soar. The effect of this drug is very surprising and dramatic, so the patients and activists in the medical world call it divine medicine.

The need for raw materials to synthesize steroid-derived drugs continues to increase along with the increasing use of steroid compounds as drugs. The need for this raw material can be fulfilled if natural steroid sources can be utilized optimally. Natural steroids can be obtained from marine animals and plants. Cholesterol, desmosterol, sitosterol, ergosterol, fukosterol, and sargasterol have been isolated from marine algae. Poriferasterol, kalinasterol, stelasterol, and desmosterol have been isolated from marine animals [28-32].

Sea urchin gonads are one of the shallow marine natural resources that can be used to meet the needs of natural steroids. Sea urchin gonadal steroids can be obtained by extraction. One method that can be used to extract sea urchin gonadal steroids is a three-component solvent system. The advantage of this method is that it is fast, practical, and can extract samples without degradation or hydrolysis of the steroid components [33-34].

In this study, we report a new method for extracting steroids from marine natural product samples: a three-component solvent system. We found that a three-component solvent system (chloroform : methanol : water) (1 : 2 : 0.8) before and (2 : 2 : 1.8) after dilution could extract steroids in the gonads of sea urchins (*Diadema Setosum* Leske). The type of steroid

found was cholesterol (5-kolesten-3β-ol) with a level of 5.06%. This indicates that a three-component solvent system can be used to extract steroids from marine natural products.

2. Materials and Methods

2.1. Apparatus and materials.

The tools used in this study were analytical balance (Explorer Ohaus), blender (Sharp), Buchner funnel, separating funnel (Pyrex), measuring cup (Pyrex), rotary vacuum evaporator (BUCHI Rotavapor™ series R-300), chamber (Pyrex), cutter (Joyko), scissors (Joyko), ruler (Butterfly), 2B pencil (Fiber Castel), capillary tube, UV lamp (UVG-58), chemical beaker (Pyrex), desiccator, dropper pipette (Pyrex) , mercury thermometer (^oC), chromatographic column (Pyrex), Electrothermal (IA9100 series), Erlenmeyer (Pyrex), refrigerator (Sharp SJ-IS60M-SL), and oven (Sharp EO-28LP). The tools used for sample characterization were a UV-VIS spectrophotometer (Genesys 20), FTIR Shimadzu® (series Prestige-21) and FTNMR Jeol (series JNM-MY500).

The materials used in this study were the gonads of sea urchins (*Diadema Setosum* Leske), technical and p.a. chloroform (Merck), technical and p.a. methanol (Merck), aquabidest (Onelab Waterone), 10% KOH, n-hexane p.a. (Merck), ethyl acetate p.a. (Merck), concentrated sulfuric acid p.a. (Merck), Liebermann-Burchad (LB) reagent, universal indicator, silica gel G.60 (50-100) mesh ASTM (Merck), silica gel G.60 GF_{254} (Merck), plastic TLC plate (40 x 80 mm) with a thickness of 0.25 mm silica gel G/UV_{254} with fluorescence indicator (Merck), aluminum TLC plates (20 x 20 cm) with a thickness of 0.25 mm silica gel G.60 GF_{254}, glass TLC plates (20 x 20 cm) with thickness of 0.5-2.0 mm silica gel G.60 GF_{254}, aluminum foil (Bagus), and plastic wrap (Total).

2.2. Extraction.

The gonads of fresh sea urchins (2.1 kg) were blended for 45 minutes with a mixed solvent (chloroform : methanol : water) (1 : 2 : 0.8 L). The extract was diluted by adding 2.1 L of water; then, the extract was blended for 25 minutes. The extract was filtered using a Buchner funnel. The first filtrate was put into the Erlenmeyer; then, the residue was blended again for 25 minutes after adding a mixed solvent (chloroform : methanol : water) (2 : 2 : 1.8 L). The extract was filtered using a Buchner funnel. This second filtrate is mixed with the first filtrate, while the residue is discarded [35].

The filtrate was allowed to stand for 24 hours until two layers were formed, namely the chloroform layer and the methanol-water layer. The two layers are separated by a separatory funnel. The first chloroform layer was collected in an Erlenmeyer, while the methanol-water layer was added to chloroform (1.05 L) and then shaken. The mixture was left for 12 hours until two layers were formed. The chloroform layer was separated from the methanol-water layer using a separatory funnel. This second chloroform layer is mixed with the first chloroform layer, while the methanol-water layer is discarded. The chloroform extract was evaporated at 61^oC at a speed of 65-90 rpm until a concentrated ester-sterol extract was obtained [35].

2.3. Steroid Qualitative Test.

Concentrated ester-sterol extract dissolved in chloroform. The existence of steroids in liquid extracts was tested for color with Liebermann-Burchad (LB) stain spotting reagent and concentrated sulfuric acid [35].

2.4. Saponification.

Concentrated ester-sterol extract dissolved in chloroform. The liquid extract was saponified with 10% KOH in methanol and heated at 65ºC for 2 hours to boil. To find out whether saponification has occurred (the solution is alkaline), the liquid extract is tested for pH before and after saponification. The hydrolyzate was allowed to stand for 24 hours until a precipitate formed. The filtrate is separated from the residue by decantation. The filtrate was evaporated at 65ºC at a speed of 65-90 rpm until a concentrated sterol extract was obtained, while the residue was removed [35].

2.5. TLC profiling.

Concentrated sterol extract (0.1 g) was dissolved in *n*-hexane (1 mL). Liquid extracts were tested by thin layer chromatography (TLC) with various types and eluent ratios to see the stain patterns of steroid compounds contained in the extracts. The eluent system used was *n*-hexane (100%), a mixture of *n*-hexane and ethyl acetate in various ratios, and ethyl acetate (100%). The results of the TLC test separation were analyzed with a UV lamp LB stain reagent, and concentrated sulfuric acid. The eluent composition, which shows a good stain separation pattern, will be used as a reference in the fractionation process [35].

2.6. Fractionation.

Silica gel G.60 (50-100 mesh) ASTM and silica gel G.60 GF_{254} (4 : 1 g) were put into the column, then compacted and eluted with *n*-hexane. The upper surface of the silica gel in the column is covered with filter paper. Concentrated sterol extract (1 g) impregnated with silica gel (4 g) was added to the column. Concentrated sterol extracts were eluted with *n*-hexane (100%) eluent, a mixture of solvents (*n*-hexane : ethyl acetate) (15 : 1), (12 : 1), (9 : 1), (8 : 1), (6 : 1), (5 : 1), (4 : 1), and ethyl acetate (100%). The elution results were accommodated in a bottle with a volume of 25 mL. Every 1 bottle is referred to as 1 fraction. Each fraction was tested by TLC using eluent (*n*-hexane : ethyl acetate) (4 : 1). Fractions that have the same Rf value are combined and evaporated at a temperature of 69-77ºC with a speed of 65-90 rpm until a concentrated extract is obtained [35].

Compound components in the combined fractions that still have more than one spot are separated by preparative TLC. The concentrated extract of each combined fraction is dissolved in ethyl acetate. The liquid extract of each combined fraction was spotted on a glass plate (20 x 20 cm), which had been activated at 120ºC for 1 hour. The chromatogram was eluted with a solvent system (n-hexane : ethyl acetate) (12 : 1) and (2 : 1). The eluent was allowed to swell until it reached 17 cm from the boundary of the spotting. The chromatogram was removed and allowed to dry at room temperature [35].

The fractions on the chromatogram were marked with the help of a UV lamp. These fractions were scraped and extracted with ethyl acetate solvent. The filtrate is separated from the stationary phase by filtration. The filtrate was tested by TLC and the residue was discarded. Fractions that have the same Rf value are combined and evaporated at a temperature of 69-77^{o}C with a speed of 65-90 rpm until a concentrated extract is obtained [35].

2.7. Purification.

White crystals dissolved in methanol were then put in the refrigerator for 24 hours. The white crystals that formed were immediately separated from the filtrate by filtration. The white crystals were recrystallized with methanol until pure crystals were formed. Pure crystals are dried in an oven at 40^{o}C. Pure dry crystals were weighed and tested for purity by one-dimensional (1D) and two-dimensional (2D) TLC tests and melting point tests [35].

A purity test with 1D TLC was carried out using *n*-hexane (100%) eluent, a mixture of solvents (*n*-hexane : ethyl acetate) (1 : 1), (2 : 1), (3 : 1), (4 : 1) , (5 : 1), and ethyl acetate (100%). The purity test with 2D TLC was carried out by spotting the sample on a TLC plate (20 x 20 cm) at a distance of 3 cm from one corner. The TLC plate was eluted with a solvent system (*n*-hexane : ethyl acetate) (4 : 1). The solvent was allowed to swell until it reached 14 cm from the spotting limit. The TLC plate was lifted and rotated 90^{o} until the separation band from the result of the first swelling was located at the bottom of the TLC plate, then a second expansion was carried out using eluent (benzene : ethyl acetate) (4 : 1). The purity test with the melting point test is carried out by measuring the melting point of pure crystals using an electrothermal tool [35].

2.8. Determination of Steroid Levels by UV-VIS Spectrophotometry.

2.8.1. Determination of Maximum Wavelength ($\lambda_{maks.}$).

Standard cholesterol (50 mg) was dissolved in chloroform (100 mL). The standard solution (0.5 mg/mL; 0.5 mL) is placed in a measuring cylinder. This solution was diluted with chloroformo a volume of 5 mL. The standard solution (0.05 mg/mL) was put into a test tube, and then LB reagent (2 mL) was added. This standard solution was stored in a dark place for 30 minutes. The absorbance of this standard solution is measured at a wavelength of 550-700 nm [35].

2.8.2. Making a Calibration Curve.

The standard solution (0.5 mg/mL) was pipetted successively (0.1, 0.2, 0.3, 0.4, 0.5 and 0.6 mL) into a test tube. Each of these standard solutions was diluted with chloroform to a volume of 5 mL. Each of these standard solutions was added LB reagent (2 mL). This standard solution was stored in a dark place for 30 minutes. The absorbance of each of these standard solutions was measured at the maximum wavelength ($\lambda_{max.}$ 630 nm) using a blank. The calibration curve is made by plotting the concentration as the x-axis and the absorbance of standard cholesterol as the y-axis. The equation of the linear regression line is determined from this calibration curve [35].

2.8.3. Determination of Steroid Levels.

Pure crystal isolate (4.6927 mg) was dissolved in chloroform (100 mL). The isolate solution (5 mL) was put into a test tube, and then LB reagent (2 mL) was added. This isolate solution was stored in a dark place for 30 minutes. The absorbance of this isolate solution was measured at the maximum wavelength (630 nm) using a blank. The absorbance value of the isolate solution is entered into the linear regression line equation to determine the steroid levels in the isolate [35].

2.9. Steroid Structure Determination.

Steroid structures were determined using UV-VIS, FTIR, (^{1}**H**, ^{13}**C**-NMR) (1D), and (HMQC, HMBC, COSY, DEPT-135/APT) (2D) spectroscopy. Physical data: 6.14% yield; content 3.15%; melting point 147.8-149.7°C; TLC (SiO_2, *n*-hexane : ethyl acetate = 4 : 1 v/v, Rf = 0.40). UV-VIS data (Genesys 20) $\lambda_{max.}^{ethanol}$ (nm): 272.0, 282.0, 293.8, 327.3; $\lambda_{max.}^{ethanol+NaOH}$ (nm): 272.0, 282.0, 293.8, 322.5, 339.4. FTIR data (KBr) $\nu_{max.}$ (cm^{-1}): 3400 (free OH), 2935 and 2900 (C-H str aliphatic), 1700 (C=C str alkene tetrasubstituted), 1650 (C=C str alkene endocyclic), 1435 (C-H def alkenes), 1460 (CH_2 str methylene), 1450 (CH_3 str angular methyl), 1360 and 1330 (CH str geminal dimethyl terminal), and 1050 (C-O str), 1005 and 800 (OOP C-H def alkenes).

^{1}**H**-NMR 1D data (500 MHz, $CDCl_3$) δ_H (ppm): 5.41 [(t, 1**H**) (C**H**-6)], 3.50 [(s, 1**H**) (C**H**-3)], 1.48 [(s, 1**H**) (C**H**-8)], 1.35 [(s, 1**H**) (C**H**-20)], 1.15 [(s, 1**H**) (C**H**-25)], 1.08 [(s, 1**H**) (C**H**-17)], 1.05 [(s, 1**H**) (C**H**-14)], 0.93 [(s, 1**H**) (C**H**-9)], 2.27 [(d, 2**H**) (C**H$_2$**-4)], 2.02 [(t, 2**H**) (C**H$_2$**-7)], 1.98 [(t, 2**H**) (C**H$_2$**-12)], 1.85 [(q, 2**H**) (C**H$_2$**-2)], 1.84 [(t, 2**H**) (C**H$_2$**-1)], 1.66 [(m, 2**H**) (C**H$_2$**-23)], 1.63 [(q, 2**H**) (C**H$_2$**-16)], 1.56 [(q, 2**H**) (C**H$_2$**-15)], 1.49 [(q, 2**H**) (C**H$_2$**-11)], 1.03 [(q, 2**H**) (C**H$_2$**-22)], 0.91 [(q, 2**H**) (C**H$_2$**-24)], 1.10 [(s, 3**H**) (C**H$_3$**-19)], 0.94 [(d, 3**H**) (C**H$_3$**-21)], 0.90 [(d, 3**H**) (C**H$_3$**-27)], 0.83 [(d, 3**H**) (C**H$_3$**-26)], 0.68 [(s, 3**H**) (C**H$_3$**-18)], and 5.10 [(s, 1**H**) (CO**H**-3)].

^{13}**C**-NMR 1D data (500 MHz, $CDCl_3$) δ_C (ppm): 37.4 [(**C**H_2) (**C**-1)], 31.4 [(**C**H_2) (**C**-2)], 71.9 [(**C**HOH) (**C**-3)], 42.4 [(**C**H_2) (**C**-4), 140.9 [(**C**-quaternary) (**C**-5)], 121.9 [(**C**H) (**C**-6)], 32.2 [(**C**H_2) (**C**-7)], 35.7 [(**C**H) (**C**-8)], 50.3 [(**C**H) (**C**-9)], 36.6 [(**C**-quaternary) (**C**-10)], 21.2 [(**C**H_2) (**C**-11)], 39.9 [(**C**H_2) (**C**-12)], 42.4 [(**C**-quaternary) (**C**-13)], 56.9 [(**C**H) (**C**-14)], 24.4 [(**C**H_2) (**C**-15)], 28.4 [(**C**H_2) (**C**-16)], 56.2 [(**C**H) (**C**-17)], 12.0 [(**C**H_3) (**C**-18)], 19.5 [(**C**H_3) (**C**-19)], 36.3 [(**C**H) (**C**-20)], 18.9 [(**C**H_3) (**C**-21)], 34.0 [(**C**H_2) (**C**-22)], 29.3 [(**C**H_2) (**C**-23)], 45.9 [(**C**H_2) (**C**-24)], 26.2 [(**C**H) (**C**-25)], 19.1 [(**C**H_3) (**C**-26)], and 20.0 [(**C**H_3) (**C**-27)].

HMQC 2D data (500 MHz, $CDCl_3$) [1.84 (**H**-1) → 37.4 (**C**-1)], [1.85 (**H**-2) → 31.4 (**C**-2)], [3.50 (**H**-3) → 71.9 (**C**-3)], [2.27 (**H**-4) → 42.4 (**C**-4)], [5.41 (**H**-6) → 121.9 (**C**-6)], [2.02 (**H**-7) → 32.2 (**C**-7)], [1.48 (**H**-8) → 35.7 (**C**-8)], [0.93 (**H**-9) → 50.3 (**C**-9)], [1.49 (**H**-11) → 21.2 (**C**-11)], [1.98 (**H**-12) → 39.9 (**C**-12)], [1.05 (**H**-14) → 56.9 (**C**-14)], [1.56 (**H**-15) → 24.4 (**C**-15)], [1.63 (**H**-16) → 28.4 (**C**-16)], [1.08 (**H**-17) → 56.2 (**C**-17)], [0.68 (**H**-18) → 12.0 (**C**-18)], [1.10 (**H**-19) → 19.5 (**C**-19)], [1.35 (**H**-20) → 36.3 (**C**-20)], [0.94 (**H**-21) → 18.9 (**C**-21)], [1.03 (**H**-22) → 34.0 (**C**-22)], [1.66 (**H**-23) → 29.3 (**C**-23)], [0.91 (**H**-24) → 45.9 (**C**-24)], [1.15 (**H**-25) → 26.2 (**C**-25)], [0.83 (**H**-26) → 19.1 (**C**-26)], and [0.90 (**H**-27) → 20.0 (**C**-27)].

The positions of the chemical shift values (δ) (ppm) **^{1}H**, **^{13}C**-NMR 1D, and HMQC 2D on the carbon skeleton of sea urchin (*Diadema Setosum* Leske) isolate are shown in Figure 1.

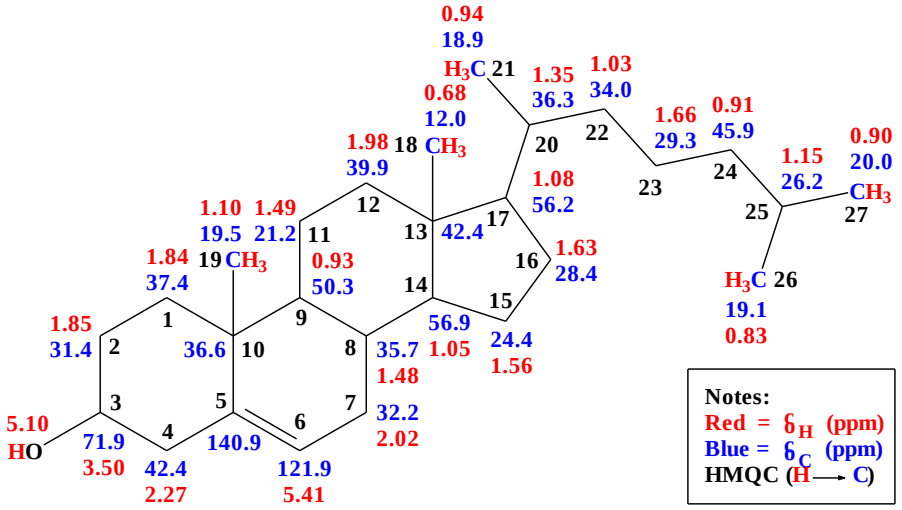

Figure 1. The position of chemical shift values (δ) (ppm) of **^{1}H, ^{13}C**-NMR 1D and [(HMQC (**H → C**)] 2D on the carbon skeleton of sea urchin (*Diadema Setosum* Leske) gonad isolates

3. Results and Discussion

3.1. Results of Extraction and Isolation of sea urchin (Diadema Setosum Leske) gonads with a Three-Component Solvent System.

The results of extraction and isolation of the gonads of sea urchins (*Diadema Setosum* Leske) with a three-component solvent system are shown in Table 1.

Table 1. Results of extraction and isolation of sea urchin (Diadema Setosum Leske) gonads with a three-component solvent system.

Sea urchin (*Diadema Setosum* Leske) Gonad Isolates							
Fraction	Amount	Rf Eluent (*n*-hexane:ethylacetate) (4:1)	Form	Color	Weight or Volume	Color Test	
						LB (Greenish blue)	H_2SO_4 (Red purple)
FA	3	0.86	Solids (powder)	White	0.0156 mg	-	-
		0.77	Solids (powder)	White	0.0264 mg	-	-
		0.66	Liquid (oil)	Yellow	3 mL	-	-
FB	1	0.49	Solids (needle crystal)	White	516.404 mg	+ (Steroids)	+ (Steroids)
FC	2	0.31	Liquid (oil)	Yellow	3 mL	-	-
		0.17	Liquid (oil)	Orange	3 mL	-	-

Table 1 shows that there are three fractions (FA, FB, FC) obtained from the extraction and isolation of the gonads of sea urchins (*Diadema Setosum* Leske) with a three-component solvent system. Of these three fractions, only the FB fraction was positive for steroids. The white crystals of the FB fraction (516,404 mg) were tested for purity by 2D TLC and melting point test. The first development using the eluent *n*-hexane : ethyl acetate (4 : 1) obtained an Rf of 0.49. The second development using the eluent benzene: ethyl acetate (4 : 1) obtained an

Rf of 0.57. The results of testing the melting point of the white crystals of the FB fraction obtained a melting point range of 147.8-149.7°C. Therefore, white crystals of the FB fraction from sea urchin (*Diadema Setosum* Leske) gonad isolates were considered sufficiently pure.

3.2. Characterization of sea urchin (Diadema Setosum Leske) gonad isolates by UV-VIS Spectrophotometer.

Figure 2 shows the UV-VIS spectrum of sea urchin (Diadema Setosum Leske) gonad isolates.

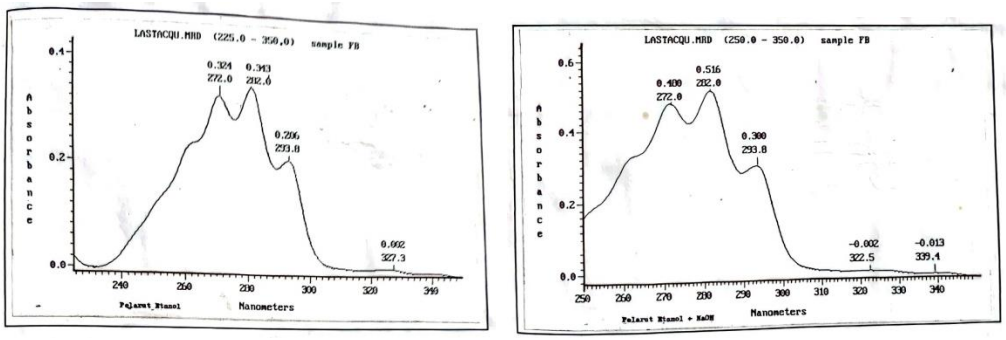

(A) (B)

Figure 2. The UV-VIS spectrum of sea urchin (Diadema Setosum Leske) gonad isolates; (A) In ethanol solvent; (B) In ethanol + NaOH solvent

The results of the UV-VIS spectrum interpretation of sea urchin (*Diadema Setosum* Leske) gonad isolates extracted with a three-component solvent system are shown in Table 2.

Table 2. The results of UV-VIS spectrum interpretation of sea urchin (*Diadema Setosum* Leske) gonad isolates

Solvent Type				Transition Type	Chromophore Type	Shift Type
Ethanol		Ethanol + NaOH				
$\lambda_{max.}$ (nm)	$A_{max.}$	$\lambda_{max.}$ (nm)	$A_{max.}$			
272.0	0.324	272.0	0.480	**n → σ***	—C—Ö— (isolated)	-
282.0	0.343	282.0	0.516	**π → σ***	C=C (isolated)	-
293.8	0.206	293.8	0.300	**π → π***	C=C (isolated)	-
327.3	0.002	322.5	-0.002	**n → σ***	—Ö—H (isolated)	Hypochromic (blue shift)

The UV-VIS spectrum of the isolate (Figure 2) shows that there are 4 (four) maximum absorption peak bands in ethanol solvent at $\lambda_{max.}$ (nm): 272.0; 282.0; 293.8; and 327.3. After the addition of NaOH in ethanol solvent, it was also found that there were 4 (four) maximum absorption peak bands at $\lambda_{max.}$ (nm): 272.0; 282.0; 293.8; and 322.5. The absorption band at $\lambda_{max.}$ 272.0 nm indicates the presence of **n → σ*** transition from the chromophore of the isolated oxy-carbon (-**C**-**O**-). The absorption band at $\lambda_{max.}$ 282.0 nm indicates the presence of **π → σ*** transition from the chromophore of the isolated alkene group (>**C**=**C**<). The absorption

band at $\lambda_{max.}$ 293.8 nm indicates the presence of $\pi \rightarrow \pi^*$ transition from the chromophore of the isolated alkene group (>**C=C**<). These three absorption bands did not change after the addition of NaOH in ethanol solvent. This shows that increasing the polarity of the solvent does not cause a shift in $\lambda_{max.}$, but only increases the absorption intensity, namely a shift towards $A_{max.}$ bigger.

The absorption band at $\lambda_{max.}$ 327.3 nm indicates the presence of $n \rightarrow \sigma^*$ transition from the chromophore of the isolated hydroxyl group (-**OH**). This absorption band changes to $\lambda_{max.}$ 322.5 nm after the addition of NaOH in ethanol solvent. This shows that increasing the polarity of the solvent causes a smaller shift towards the $\lambda_{max.}$ is known as a blue shift or hypochromic effect. This blue shift occurs because the **H** atom of the cyclohexanol **OH** group (substituent) chromophore reacts with **NaOH** to form its sodium salt and a water molecule (Figure 3).

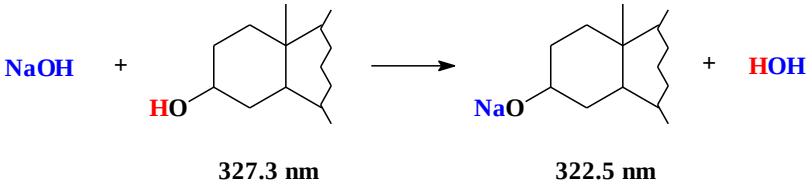

Figure 3. Blueshift (hypsochromic effect) of the **OH** group chromophore after the addition of **NaOH** in ethanol solvent

3.3. Characterization of sea urchin (Diadema Setosum Leske) gonad isolates by FTIR.

Figure 4 shows the FTIR spectrum of sea urchin (Diadema Setosum Leske) gonad isolates.

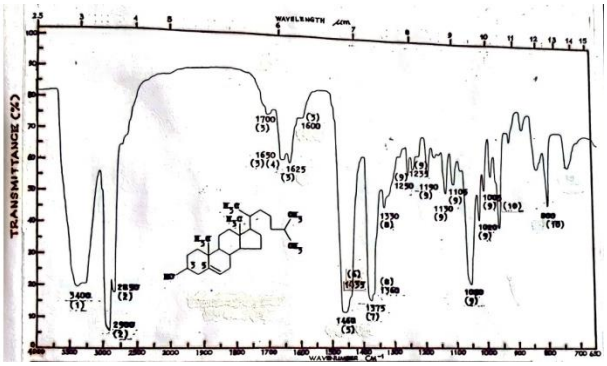

Figure 4. The FTIR spectrum of sea urchin (Diadema Setosum Leske) gonad isolates

The results of the FTIR spectrum interpretation of sea urchin (*Diadema Setosum* Leske) gonad isolates extracted with a three-component solvent system are shown in Table 3.

Table 3. The results of the FTIR spectrum data interpretation of sea urchin (*Diadema Setosum* Leske) gonad isolates.

No	Frequency (cm^{-1}) and Intensities		Frequency Ranges (cm^{-1}) and Intensities*	Group or Class	Remarks
	Cholesterol	Isolate	References		
1	3412 (s)	3400 (s)	3400 - 3300 (s)	Alcohols ROH	O-H stretch, broadband
2	1431 (s)	1435 (s) and 1360 (s)	1450 - 1350 (m)		O-H in-plane bend
3	1040 (s)	1050 (s)	1150 - 1050 (m-s)		C-O antisym stretch
4	957 (m)	955 (m) and 800 (m)	970 - 800 (s)		C-C-O sym stretch
5	2956 (s)	2935 (s) and 2900 (s)	2980 - 2800 (vs)	Alkanes	C-H stretch

No	Frequency (cm^{-1}) and Intensities		Frequency Ranges (cm^{-1}) and Intensities*	Group or Class	Remarks
	Cholesterol	Isolate	References		
				RH	
6	2866 (s)	2850 (s)	2980 - 2850 (m)	Alkyl R	C-H stretch
7	1452 (s)	1450 (s)	1470 - 1430 (m-s)	Methyl $-CH_3$	C-H stretch, CH_3- sym def or angular
8	1379 (s)	1375 (s)	1390 - 1370 (m-s)		C-H stretch, CH_3- antisym def
9	1367 (s)	1360 (s) and 1330 (m)	1300 - 1365 (m-s)		C-H stretch geminal dimethyl terminal
10	1462 (s)	1460 (s)	1470 - 1450 (m)	Methylene	C-H stretch, $-CH_2$- deformation
11	731 (m)	730 (m)	740 - 720 (w)	$-CH_2$-	C-H stretch, $-CH_2$- rocking
12	3253 (s)	3250 (s)	3290 - 2850 (m)	Alkenes	C-H stretches in alkenes
13	1705 (w)	1700 (w)	1700 - 1670 (w)	>C=C<	C=C stretch, alkene tetrasubst
14	1664 (s)	1650 (m)	1675 - 1600 (m-s)		C=C stretch, endocyclic alkenes
15	1335 (m)	1330 (m) and 1235 (m)	1450 - 1200 (vs)		C-H in-plane deformation
16	1003 (m)	1005 (m) and 800 (m)	1005 - 800 (m)		C-H out-of-plane def alkena

◦Notes: vs = *very strong*; v = *variable*; s = *strong*; m = *medium*; w = *weak*.
*Sources: [36-38]

FTlR (KBr) spectrum data of sea urchin (*Diadema Setosum* Leske) gonad isolate, and standard cholesterol are shown in Table 3. The FTIR spectrum of the isolate (Figure 4) shows an absorption band at wave number 3400 cm^{-1}, which indicates the presence of free **OH** groups. The presence of the **OH** group is also supported by the presence of an absorption peak at 1050 cm^{-1} for the **C-O** stretching vibration. The assumption that the isolate has a free **OH** group is also supported by the occurrence of a blue shift (hypsochromic effect) in the UV-VIS spectrum of the isolate (Table 2). Other absorption peaks at 2935 and 2900 cm^{-1} indicate the existence of aliphatic **C-H** stretching, which is supported by the presence of absorption at 1460 cm^{-1} (**CH_2**), 1450 cm^{-1} (**CH_3** angular), 1360 cm^{-1} and 1330 cm^{-1} (**CH_3** geminal dimethyl terminal). The absorption peaks at 1650 cm^{-1} and 1700 cm^{-1} indicated the presence of olefin groups (>**C=C**<) from endocyclic and tetrasubstituted alkenes. The assumption that the isolate has an olefin group (>**C=C**<) from an alkene is also supported by the presence of $\pi \rightarrow \sigma^*$ and $\pi \rightarrow \pi^*$ transitions at $\lambda_{max.}$ 282.0 nm and 293.8 nm from the chromophore of the isolated olefin group (>**C=C**<) in the UV-VIS spectrum of the isolated compound (Table 2). The absorption peaks of this isolate are very similar to the absorption peaks shown by standard cholesterol (Table 3).

3.4. Characterization of sea urchin (Diadema Setosum Leske) gonad isolates by ^1H, ^{13}C-NMR, DEPT-135/APT, HMQC, HMBC, and COSY.

Figure 5 shows the **^1H**-NMR 1D (500 MHz, $CDCl_3$) spectrum of sea urchin (Diadema Setosum Leske) gonad isolates.

Spectral data of the **^1H**-NMR 1D (500 MHz, $CDCl_3$) of sea urchin (*Diadema Setosum* Leske) gonad isolates and standard cholesterol are shown in Table 4. The **^1H**-NMR spectrum of the isolate (Figure 5) shows the presence of methine (**CH**) proton signals in the regions of 6 δ_H (ppm): 5.41 [(t, 1**H**) (C**H**-6)], 3.50 [(s, 1**H**) (C**H**-3)], 1.48 [(s, 1**H**) (C**H**-8)], 1.08 [(s, 1**H**) (C**H**-17)], 1.05 [(s, 1**H**) (C**H**-14)], and 0.93 [(s, 1**H**) (C**H**-9)]. The methylene (**CH_2**) proton signal appears in the regions of 8 δ_H (ppm): 2.27 [(d, 2**H**) (C**H_2**-4)], 2.02 [(t, 2**H**) (C**H_2**-7)], 1.98 [(t, 2**H**) (C**H_2**-12)], 1.85 [(q, 2**H**) (C**H_2**-2)], 1.84 [(t, 2**H**) (C**H_2**-1)], 1.63 [(q, 2**H**) (C**H_2**-16)], 1.56 [(q, 2**H**) (C**H_2**-15)], and 1.49 [(q, 2**H**) (C**H_2**-11)]. The methyl (**CH_3**) proton signal occurs in the regions of 2 δ_H (ppm): 0.68 [(s, 3**H**) (C**H_3**-18)] and 1.10 [(s, 3**H**) (C**H_3**-19)]. The

free hydroxyl (O**H**) group proton signal appears in the region of δ_H (ppm) 5.10 [(s, 1**H**) (CO**H**-3)].

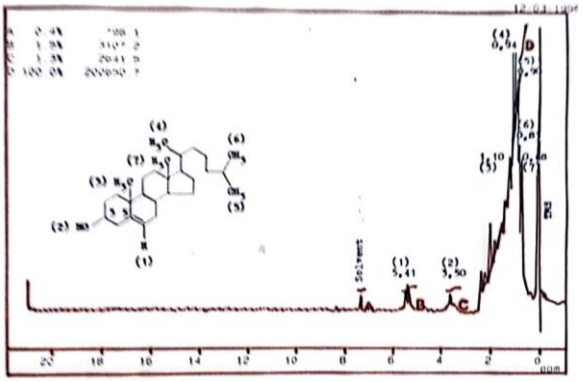

Figure 5. The ^{1}**H**-NMR 1D (500 MHz, $CDCl_3$) spectrum of sea urchin (Diadema Setosum Leske) gonad isolates.

The proton signals indicated the presence of a steroid skeleton substituted by two angular methyl groups (C**H$_3$**-18) and (C**H$_3$**-19) and one hydroxyl group (CO**H**-3) (Figure 7). In the aliphatic region, there are also several proton signals indicating the presence of an alkane unit. The methine (C**H**) proton signal occurs in the regions of 2 δ_H (ppm): 1.35 [(s, 1**H**) (C**H**-20)] and 1.15 [(s, 1**H**) (C**H**-25)]. The methylene **(CH_2)** proton signal appears in the regions of 3 δ_H (ppm): 1.66 [(m, 2**H**) (C**H$_2$**-23)], 1.03 [(q, 2**H**) (C**H$_2$**-22)], and 0.91 [(q, 2**H**) (C**H$_2$**-24)]. The methyl **(CH_3)** proton signal appears in the regions of 3 δ_H (ppm): 0.94 [(d, 3**H**) (C**H$_3$**-21)], 0.90 [(d, 3**H**) (C**H$_3$**-27)], and 0.83 [(d, 3**H**) (C**H$_3$**-26)]. These eight signal protons constitute the alkyl (C_8H_{17}) skeleton of the steroid side chain (Figure 7).

Spectral data of ^{1}**H,** ^{13}**C**-NMR 1D (500 MHz, $CDCl_3$), HMQC, HMBC, COSY, and DEFT-135/APT 2D (500 MHz, $CDCl_3$) of sea urchin (*Diadema Setosum* Leske) gonad isolates and standard cholesterol are shown in Table 4.

Table 4. Chemical shift value (δ) ^{1}H, ^{13}C-NMR, HMQC, HMBC, COSY, DEPT-135/APT of standard cholesterol and sea urchin (*Diadema Setosum* Leske) gonad isolates.

^{1}H, ^{13}C-NMR					HMQC (H → C) Directly Attached δ_C (ppm)	HMBC (H → C) Neighbour Carbons δ_C (ppm)	COSY (H → H) Neighbour Protons δ_H (ppm)	DEPT-135/APT		Groups
C, H Position	δ_C (ppm)		δ_H (ppm) (ΣH, multi) (*J* Hz)					C + δ_C (ppm)	C – δ_C (ppm)	
	Cholesterol	Isolate	Cholesterol	Isolate						
1	37.3	37.4	1.82 (2**H**, *m*)	1.84 (2**H**, *m*)	37.4	C-4			**37.4**	**-CH$_2$-**
2	31.8	31.4	1.83 (2**H**, *m*)	1.85 (2**H**, *m*)	31.4	C-3, C-10	H-3		**31.4**	**-CH$_2$-**
3	71.9	71.9	3.52 (1**H**, *m*) 5.12 (1**H**, *s*)	3.50 (1**H**, *m*) 5.10 (1**H**, *s*)	71.9	C-5	H-4	**71.9**		**C-H** **C-OH**
4	42.4	42.4	2.25 (2**H**, *m*)	2.27 (2**H**, *m*)	42.4	C-6, C-10			**42.4**	**-CH$_2$-**
5	140.9	140.9	-	-	-			**140.9**		**>C=C<**
6	121.8	121.9	5.34 (1**H**, *t*) (4.9)	5.41 (1**H**, *t*) (4.9)	121.9	C-4, C-8, C-10	H-7	**121.9**		**>C=C<**
7	32.0	32.2	2.00 (2**H**, *m*)	2.02 (2**H**, *m*)	32.2				**32.09**	**-CH$_2$-**
8	35.5	35.7	1.46 (1**H**, *m*)	1.48 (1**H**, *m*)	35.7			**35.7**		**C-H**
9	50.3	50.3	0.91 (1**H**, *m*)	0.93 (1**H**, *m*)	50.3		H-11	**50.3**		**C-H**
10	36.6	36.6	-	-	-			**36.6**		**>C<**
11	21.1	21.2	1.47	1.49	21.2				**21.2**	**-CH$_2$-**

^{1}H, ^{13}C-NMR					HMQC (H → C) Directly Attached δ_C (ppm)	HMBC (H → C) Neighbour Carbons δ_C (ppm)	COSY (H → H) Neighbour Protons δ_H (ppm)	DEPT-135/APT		Groups
C, H Position	δ_C (ppm)		δ_H (ppm) (ΣH, multi) (*J* Hz)					C + δ_C (ppm)	C – δ_C (ppm)	
	Cholesterol	Isolate	Cholesterol	Isolate						
			(2**H**, *m*)	(2**H**, *m*)						
12	39.9	39.9	1.96 (2**H**, *m*)	1.98 (2**H**, *m*)	39.9	C-9, C-14			**39.9**	**-CH_2-**
13	42.4	42.4	-	-	-			**42.4**		**>C<**
14	56.8	56.9	1.03 (1**H**, *m*)	1.05 (1**H**, *m*)	56.9			**56.9**		**C-H**
15	24.3	24.4	1.55 (2**H**, *m*)	1.56 (2**H**, *m*)	24.4				**24.4**	**-CH_2-**
16	28.2	28.4	1.61 (2**H**, *m*)	1.63 (2**H**, *m*)	28.4				**28.4**	**-CH_2-**
17	56.2	56.2	1.07 (1**H**, *m*)	1.08 (1**H**, *m*)	56.2		H-20	**56.2**		**C-H**
18	11.9	12.0	0.67 (3**H**, *s*)	0.68 (3**H**, *s*)	12.0	C-12, C-13, C-17		**12.0**		**-CH_3**
19	19.8	19.5	1.08 (3**H**, *s*)	1.10 (3**H**, *s*)	19.5	C-1, C-9, C-10		**19.5**		**-CH_3**
20	36.2	36.3	1.33 (1**H**, *m*)	1.35 (1**H**, *m*)	36.3			**36.3**		**C-H**
21	18.8	18.9	0.92 (3**H**, *d*) (6.7)	0.94 (3**H**, *d*) (6.7)	18.9	C-17, C-20, C-22		**18.9**		**-CH_3**
22	34.0	34.0	1.01 (2**H**, *m*)	1.03 (2**H**, *m*)	34.0	C-21			**34.0**	**-CH_2-**
23	29.3	29.3	1.65 (2**H**, *m*)	1.66 (2**H**, *m*)	29.3		H-24		**29.3**	**-CH_2-**
24	50.3	45.9	0.92 (2**H**, *m*)	0.91 (2**H**, *m*)	45.9				**45.9**	**-CH_2-**
25	26.2	26.2	1.13 (1**H**, *m*)	1.15 (1**H**, *m*)	26.2		H-27	**26.2**		**C-H**
26	18.8	19.1	0.81 (3**H**, *d*)	0.83 (3**H**, *d*)	19.1			**19.1**		**-CH_3**
27	19.8	20.0	0.89 (3**H**, *d*)	0.90 (3**H**, *d*)	20.0	C-24, C-25		**20.0**		**-CH_3**

Figure 6 shows the **^{13}C**-NMR 1D (500 MHz, $CDCl_3$) and DEPT-135/APT 2D spectrum of sea urchin (Diadema Setosum Leske) gonad isolates.

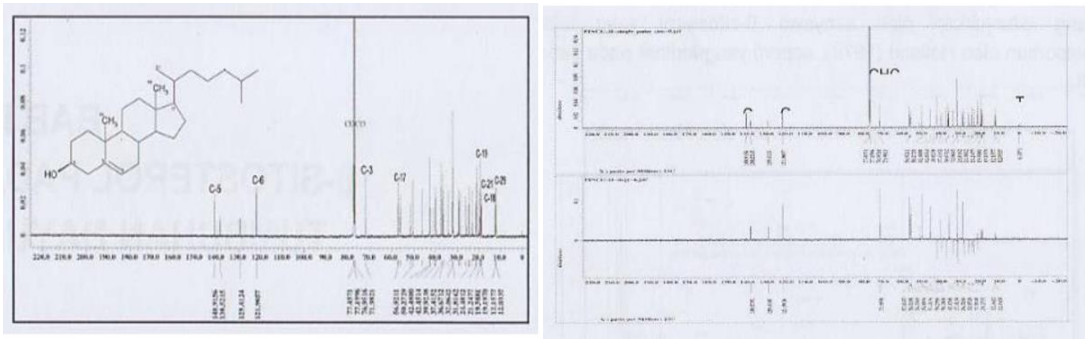

(A) (B)

Figure 6. The (A) **^{13}C**-NMR 1D (500 MHz, $CDCl_3$); and (B) DEPT-135/APT 2D spectrum of sea urchin (Diadema Setosum Leske) gonad isolates

Spectral data of the **^{13}C**-NMR 1D (500 MHz, $CDCl_3$) and DEPT-135/APT 2D of sea urchin (*Diadema Setosum* Leske) gonad isolates and standard cholesterol are shown in Table 4. The **^{13}C**-NMR 1D spectrum of the isolated compound (Figure 6A) shows the presence of 27 signals representing the 27 carbons (Figure 7). To find out the type of carbon group that the isolate has, the measurement is continued by using DEPT-135/APT 2D analysis. The DEPT-135/APT 2D spectrum of the isolated compound (Figure 6B and Table 4) showed 16 positive carbon signals consisting of 7 methine carbons (**C**H) at δ_C (ppm): [71.9 (**C**-3), 35.7 (**C**- 8), 50.3

(**C**-9), 56.9 (**C**-14), 56.2 (**C**-17), 36.3 (**C**-20), and 26.2 (**C**-25)], 5 methyl carbons (**C**H_3) at δ_C (ppm): [12.0 (**C**-18), 19.5 (**C**-19), 18.9 (**C**-21), 19.1 (**C**-26), and 20.0 (**C**-27)], 2 alkene carbons (>**C**=**C**<) at δ_C (ppm): [140.9 (**C**-5) and 121.9 (**C**-6)], and 2 quaternary carbons (>**C**<) at δ_C (ppm): [36.6 (**C**-10) and 42.4 (**C**-13)]. The DEPT-135/APT 2D spectrum of the isolated compound (Figure 6B and Table 4) also showed 11 negative carbon signals from methylene carbon (**C**H_2) at δ_C (ppm): [37.4 (**C**-1), 31.4 (**C**-2) , 42.4 (**C**-4), 32.2 (**C**-7), 21.2 (**C**-11), 39.9 (**C**-12), 24.4 (**C**-15), 28.4 (**C**-16), 34.0 (**C**-22), 29.3 (**C**-23), and 45.9 (**C**-24)]. The DEPT-135/APT 2D spectrum of the isolated compound (Figure 6B and Table 4) also showed the presence of carbon oxy at δ_C 71.9 ppm (**C**-3).

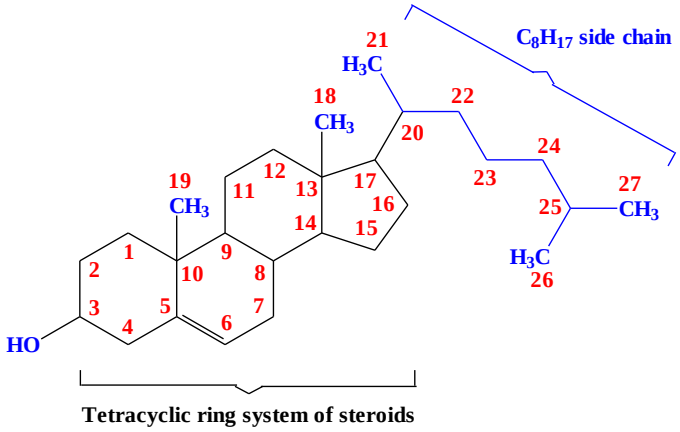

Figure 7. The steroid carbon skeletons of sea urchin (*Diadema Setosum* Leske) gonad isolates.

The twenty-seven carbon signals form the tetracyclic ring system of the steroid skeleton with one double bond (>**C**=**C**<) on the **C**-5 and **C**-6 atoms. The **C**-17 atom of the steroid skeleton is attached to the **C**-20 atom of the side chain of the C_8H_{17} alkyl unit of the alkane (Figure 7). The ^{13}**C**-NMR spectroscopy data of the isolated compounds was significant, with the absorption peaks indicated by the standard cholesterol compounds (Table 4).

Spectral data of the HMQC 2D (500 MHz, $CDCl_3$) of sea urchin (*Diadema Setosum* Leske) gonad isolates and standard cholesterol are shown in Table 4. HMQC is an analysis in which the resulting spectrum is in the form of contours (spots) that show a direct correlation between the proton (^{1}**H** -NMR) signal and a carbon (^{13}**C**-NMR) signal. The HMQC (**H** → **C**) spectra of the isolates (Table 4) show a direct correlation between the proton signal at δ_H (ppm) and the carbon signal at δ_C (ppm): [1.84 (**H**-1) → 37.4 (**C**-1)], [1.85 (**H**-2) → 31.4 (**C**-2)], [3.50 (**H**-3) → 71.9 (**C**-3)], [2.27 (**H**-4) → 42.4 (**C**-4)], [5.41 (**H**-6) → 121.9 (**C**-6)], [2.02 (**H**-7) → 32.2 (**C**-7)], [1.48 (**H**-8) → 35.7 (**C**-8)], [0.93 (**H**-9) → 50.3 (**C**-9)], [1.49 (**H**-11) → 21.2 (**C**-11)], [1.98 (**H**-12) → 39.9 (**C**-12)], [1.05 (**H**-14) → 56.9 (**C**-14)], [1.56 (**H**-15) → 24.4 (**C**-15)], [1.63 (**H**-16) → 28.4 (**C**-16)], [1.08 (**H**-17) → 56.2 (**C**-17)], [0.68 (**H**-18) → 12.0 (**C**-18)], [1.10 (**H**-19) → 19.5 (**C**-19)], [1.35 (**H**-20) → 36.3 (**C**-20)], [0.94 (**H**-21) → 18.9 (**C**-21)], [1.03 (**H**-22) → 34.0 (**C**-22)], [1.66 (**H**-23) → 29.3 (**C**-23)], [0.91 (**H**-24) → 45.9 (**C**-24)], [1.15 (**H**-25) → 26.2 (**C**-25)], [0.83 (**H**-26) → 19.1 (**C**-26)], and [0.90 (**H**-27) → 20.0 (**C**-27)]. The HMQC correlation of sea urchin (*Diadema Setosum* Leske) gonad isolates can be seen in Table 4 and Figure 10.

Figure 8 shows the HMBC 2D (500 MHz, $CDCl_3$) spectrum of sea urchin (Diadema Setosum Leske) gonad isolates.

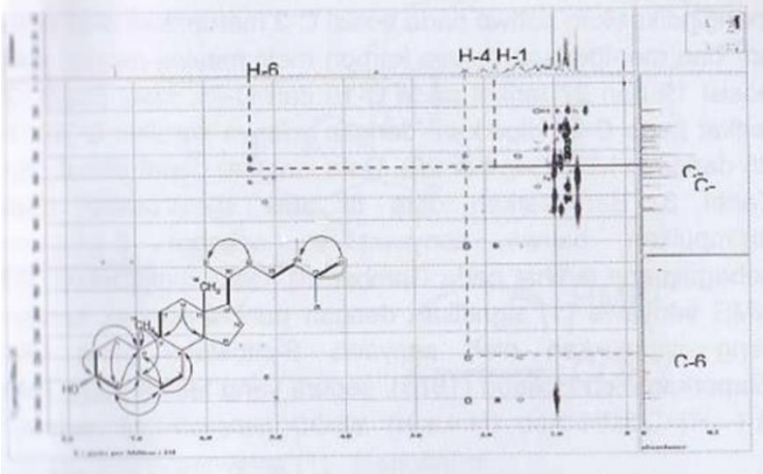

Figure 8. The HMBC 2D (500 MHz, $CDCl_3$) spectrum of sea urchin (Diadema Setosum Leske) gonad isolates.

Spectral data of HMBC 2D (500 MHz, CDCl3) of sea urchin (*Diadema Setosum* Leske) gonad isolate and standard cholesterol are shown in Table 4. The HMBC (**H** → **C**) spectrum of isolates (Figure 8) shows a long-distance correlation between the proton signal at δ_H 1.84 ppm (**H**-1) with carbon at δ_C 42.4 ppm (**C**-4), proton signal at δ_H 1.85 ppm (**H**-2) with carbon at δ_C 71.9 ppm (**C**-3) and 36.6 ppm (**C**-10), proton signal at δ_H 3.50 ppm (**H**-3) with carbon at δ_C 140.9 ppm (**C**-5), proton signal at δ_H 2.27 ppm (**H**-4) with carbon at δ_C 121.9 ppm (**C**-6) and 36.6 ppm (**C**-10), proton signal at δ_H 5.41 ppm (**H**-6) with carbon at δ_C 42.4 ppm (**C**-4), 35.7 ppm (**C**-8), and 36.6 ppm (**C**-10), proton signals at δ_H 1.98 ppm (**H**-12) with carbon at δ_C 50.3 ppm (**C**-9) and 56,9 ppm (**C**-14). Long distance correlation between the signals of methyl protons at δ_H 0.68 ppm (C**H**$_3$-18) and carbon at δ_C 39.9 ppm (**C**-12), 42.4 ppm (**C**-13), and 56.2 ppm (**C**-17) shows that the methyl on (C**H**$_3$-18) is bound to **C**-13.

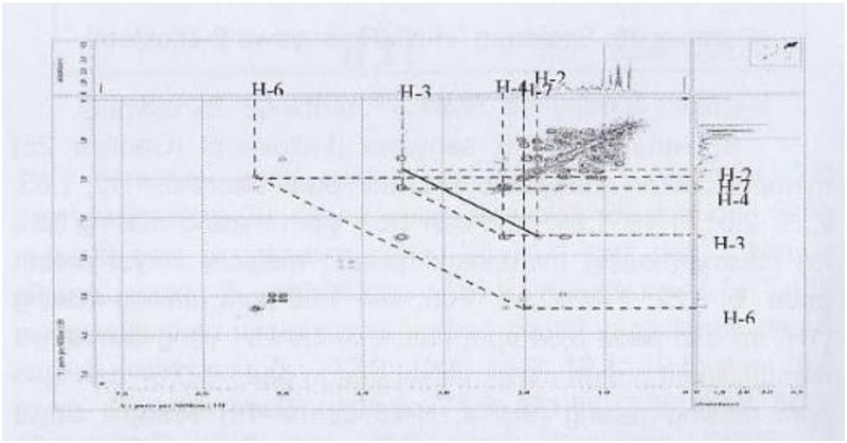

Figure 9. The COSYspectrum of sea urchin (Diadema Setosum Leske) gonad isolates.

Long distance correlation between the signals of methyl protons at δ_H 1.10 ppm (C**H**$_3$-19) and carbon at δ_C 37.4 ppm (**C**-1), 50.3 ppm (**C**-9), and 36.6 ppm (**C**-10) shows that the methyl on (C**H**$_3$-19) is bound to **C**-10. Long distance correlation between the signals of methyl protons at δ_H 0.94 ppm (C**H**$_3$-21) and carbon at δ_C 36.3 ppm (**C**-20), 56.2 ppm (**C**-17), and 34.0 ppm (**C**- 22) shows that the methyl on (C**H**$_3$-21) is bound to **C**-20. Proton signal at δ_H 1.03 ppm (**H**-22) is correlated with the distance of 2 bonds with carbon at δ_C 18.9 ppm (**C**-21). The long-distance correlation between the signals of the methyl proton at δ_H 0.90 ppm (C**H**$_3$-27) and the carbon at δ_C 45.9 ppm (**C**-24) and 26.2 ppm (**C**-25) shows that the methyl at (C**H**$_3$-27)

bound to **C**-25 which is strengthened by the COSY correlation between **H**-25 and **H**-27 (Figure 9). Figure 9 shows the COSY spectrum of sea urchin (Diadema Setosum Leske) gonad isolates.

The COSY (**H** → **H**) spectral data of sea urchin (*Diadema Setosum* Leske) gonad isolates (Figure 9 and Table 4) show a correlation between neighboring proton signals at δ_H 1.85 ppm (**H**-2) and proton at δ_H 3.50 ppm (**H**-3), proton signal at δ_H 3.50 ppm (**H**-3) with proton at δ_H 2.27 ppm (**H**-4), proton signal at δ_H 0.93 ppm (**H**-9) with proton at δ_H 1.49 ppm (**H**-11), proton signal at δ_H 1.08 ppm (**H**-17) with proton at δ_H 1.35 ppm (**H**-20), proton signal at δ_H 1.66 ppm (**H**-23) with proton δ_H 0, 91 ppm (**H**-24), and a proton signal at δ_H 1.15 ppm (**H**-25) with a proton at δ_H 0.90 ppm (**H**-27).

The HMQC, HMBC, and COSY correlations on the carbon skeletons of sea urchin (*Diadema Setosum* Leske) gonad isolates can be seen in Figure 10.

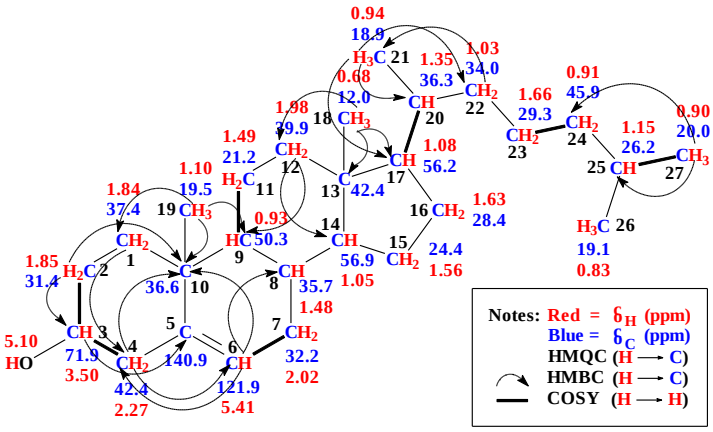

Figure 10. The HMQC, HMBC, and COSY correlations on the carbon skeletons of sea urchin (*Diadema Setosum* Leske) gonad isolates.

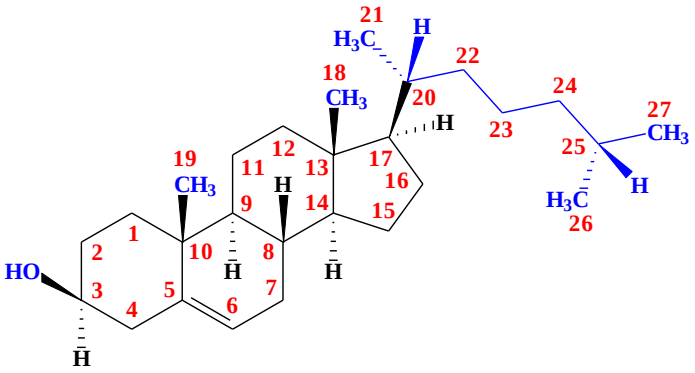

(A) Absolute configuration of cholesterol (5-cholesten-3β-ol).

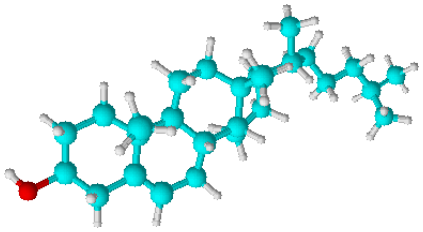

(B) 3D structure of sticks & balls of cholesterol (5-cholesten-3β-ol).

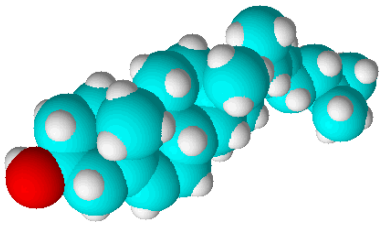

(C) 3D structure of spacefill of cholesterol (5-cholesten-3β-ol).

Figure 11. Absolute configuration and 3D structure of cholesterol (5-cholesten-3β-ol) of sea urchin (*Diadema Setosum* Leske) gonad isolates.

Based on the description and spectroscopic data above, it can be concluded that the isolated compound is cholesterol (5-cholesten-3β-ol). Cholesterol contains a tetracyclic skeleton modified to include an alcohol function group at **C**-3, a double bond at **C**-5, methyl groups at **C**-10 and **C**-13, and a C_8H_{17} side chain at **C**-17 [39-41] (Figure 11). This is also supported by spectroscopic data of standard cholesterol compounds very similar to the absorption peaks shown by the gonad isolate of sea urchins (*Diadema Setosum* Leske) (Table 4).

3.5. Determination of steroid levels of sea urchin (Diadema Setosum Leske) gonad isolates by UV-VIS spectrophotometry.

The results of measuring the absorbance of a standard cholesterol solution of 0.05 mg/mL at a wavelength of 550 – 700 nm obtained $\lambda_{max.}$ 630 nm ($A_{max.}$ 1.853). The results of the absorbance measurement of standard cholesterol solutions of 0.01 – 0.06 mg/mL at $\lambda_{max.}$ 630 nm, and the calibration curve is presented in Figure 12.

Consentration (C) (mg/mL) x	Absorbansce (A) y
0,01	0,413
0,02	0,673
0,03	0,912
0,04	1,124
0,05	1,352
0,06	1,579

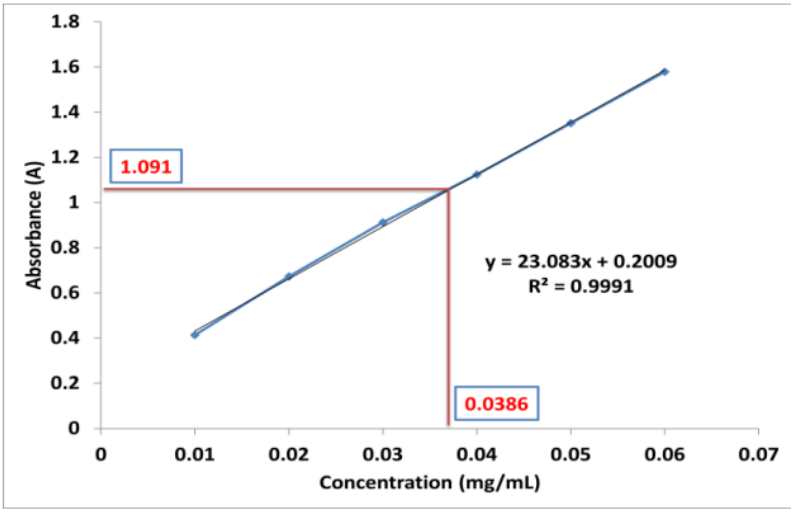

Figure 12. Standard cholesterol solution calibration curve.

The results of measuring the absorbance of the isolate solution at $\lambda_{max.}$ 630 nm obtained absorbance (A) of 1.091. If this value is entered into the regression equation on the calibration curve (Figure 12), the value for the concentration (x) of the isolate solution is 0.0386 mg/mL. So, the steroid content per 8,400 mg sample of dry gonads of sea urchins (*Diadema Setosum* Leske) is 5.06%.

4. Conclusions

Sea urchin (*Diadema Setosum* Leske) gonad steroids can be extracted with a three-component solvent system with a volume ratio of solvent (chloroform : methanol : water) (1 : 2 : 0.8) before and (2 : 2 : 1.8) after dilution. The type of steroid found in the gonads of sea urchins (*Diadema Setosum* Leske) is cholesterol (5-cholesten-3β-ol) with a content of 5.06%.

Funding

This research received no external funding.

Acknowledgments

The authors declare no acknowledgements.

Conflicts of Interest

The authors declare no conflict of interest.

References

1. Balasubramonian, B.; Selcer, K.W. The Phytochemical Curcumin Inhibits Steroid Sulfatase Activity in Rat Liver Tissue and NIH-3T3 Mouse Fibroblast Cells. *Steroids* **2023**, *191*, pp. 109163, ISSN 0039-128X, https://doi.org/10.1016/j.steroids.2022.109163
2. Ontiveros, L.A.C.; Hernández, L.L.R.; Sánchez, E.B.M.; Lozano, B.C.; Puerta, A.; Padrón, J.M.; Montiel, P.M.; Baez, J.L.V.; Smith, S.M. Synthesis, Antiproliferative Evaluation and in Silico Studies of a Novel Steroidal Spiro Morpholinone. *Steroids* **2023**, *192*, pp. 109173, ISSN 0039-128X, https://doi.org/10.1016/j.steroids.2023.109173
3. Kaneguchi, A.; Takahashi, A.; Shimoe, A.; Hayakawa, M.; Yamaoka, K.; Ozawa, J. The Combined Effects of Treadmill Exercise and Steroid Administration on Anterior Cruciate Ligament Reconstruction-Induced Joint Contracture and Muscle Atrophy in Rats. *Steroids* **2023**, *192*, pp. 109183, ISSN 0039-128X, https://doi.org/10.1016/j.steroids.2023.109183
4. Ansari, A.; Shamsuzzaman. Decoding the Binding Interaction of Steroidal Pyridines with Bovine Serum Albumin Using Spectroscopic and Molecular Docking Techniques. *Steroids* **2023**, *192*, pp. 109156, ISSN 0039-128X, https://doi.org/10.1016/j.steroids.2022.109156
5. Tran, B.N.; Okoniewski, R.; Spink, B.C.; LeMaster, D.M.; Aldous, K.M.; Spink, D.C. Androgenic Steroids in Over-the-Counter Dietary Supplements: Analysis for Association with Adverse Health Effects. *Steroids* **2023**, *193*, pp. 109199, ISSN 0039-128X, https://doi.org/10.1016/j.steroids.2023.109199
6. Goswami, M.; Priya; Jaswal, S.; Gupta, G. D.; Verma, S.K. A Comprehensive Update on Phytochemistry, Analytical Aspects, Medicinal Attributes, Specifications and Stability of Stigmasterol. *Steroids* **2023**, *196*, pp. 109244, ISSN 0039-128X, https://doi.org/10.1016/j.steroids.2023.109244
7. Jalalvand, A.R.; Rashidi, Z.; Khajenoori, M. Sensitive and Selective Simultaneous Biosensing of Nandrolone and Testosterone as Two Anabolic Steroids by a Novel Biosensor Assisted by Second Order Calibration. *Steroids* **2023**, *189*, pp. 109138, ISSN 0039-128X, https://doi.org/10.1016/j.steroids.2022.109138
8. Choi, K.Y.; Lee, H.J.; Lee, H.W.; Park, T.Y.; Heo, E.Y.; Kim, D.K.; Lee, J.K. Systemic Corticosteroid Use and Cardiovascular Risk in Patients Hospitalized for Pneumonia. *Steroids* **2023**, *191*, pp. 109161, ISSN 0039-128X, https://doi.org/10.1016/j.steroids.2022.109161
9. Miwa, T.; Kanai, R.; Kanemaru, S.I. Long-Term Exposure to High Concentration Dexamethasone in the Inner Ear via Intratympanic Administration. *Steroids* **2023**, *189*, pp. 109152, ISSN 0039-128X, https://doi.org/10.1016/j.steroids.2022.109152
10. da Silva, F.E.F.; do Ávila, F.N.; Pereira, N.M.O.; de Freitas, M.D.; Pessoa, O.D.L.; da Fonseca, A.M.; da Costa, J.G.M.; Santiago, G.M.P. Semisynthesis, in Silico Study and in Vitro Antibacterial Evaluation of Fucosterol Derivatives. *Steroids* **2023**, *189*, pp. 109137, ISSN 0039-128X, https://doi.org/10.1016/j.steroids.2022.109137
11. Xu, T.; Zhao, Q.M.; Yao, L.G.; Lan, L.F.; Li, S.W.; Guo, Y.W. Sinulasterols D–G, Four New Antibacterial Steroids from the South China Sea Soft Coral Sinularia Depressa. *Steroids* **2023**, *192*, pp. 109182, ISSN 0039-128X, https://doi.org/10.1016/j.steroids.2023.109182
12. Wang, X.Y.; Jiang, S.; Liu, Y. Anti-Diabetic Effects of Fungal Ergosta-4,6,8(14),22-tetraen-3-one from Pholiota Adiposa. *Steroids* **2023**, *192*, pp. 109185, ISSN 0039-128X, https://doi.org/10.1016/j.steroids.2023.109185
13. Elawad, M.A.; Elnour, M.; Elkhalifa, M.; Hamdoon, A.A.E.; Salim, L.H.M.; Ahmad, Z.; Ayaz, M. Natural Products Derived Steroids as Potential Anti-Leishmanial Agents: Disease Prevalence, Underlying Mechanisms and Future Perspectives, *Steroids* **2023**, *193*, pp. 109196, ISSN 0039-128X, https://doi.org/10.1016/j.steroids.2023.109196

14. Iqbal, A.; Khan, A.; Ahmedi, S.; Manzoor, N.; Siddiqui, T. Synthesis, Antifungal Evaluation, and Molecular Docking Studies of Steroidal Thiazolopyrimidines. *Steroids* **2023**, *193*, pp. 109186, ISSN 0039-128X, https://doi.org/10.1016/j.steroids.2023.109186
15. Uttu, A.J.; Sallau, M.S.; Ibrahim, H.; Iyun, O.R.A. In Silico Modelling and NMR Characterization of Some Steroids from Strychnos Innocua (Delile) Root Bark as Potential Antifungal Agents. *Steroids* **2023**, *194*, pp. 109222, ISSN 0039-128X, https://doi.org/10.1016/j.steroids.2023.109222
16. El-Shiekh, R.A.; Shalabi, A.A.; Al-Hawshabi, O.S.S.; Salkini, M.A.; Sattar, E.A. Anticholinesterase and Anti-Inflammatory Constituents from Caralluma Awdeliana, a Medicinal Plant from Yemen, *Steroids* **2023**, *193*, pp. 109198, ISSN 0039-128X, https://doi.org/10.1016/j.steroids.2023.109198
17. Aziz, A.; Wahab, A.; Siddiqui, M.; Khan, N.; Jabeen, A.; Ahmed, Z.; Choudhary, M.I. Glomerella Fusarioides-Catalyzed Structural Transformation of Steroidal Drugs Mesterolone and Methasterone, and Anti-Inflammatory Activity of Resulting Derivatives. *Steroids* **2023**, *194*, pp. 109219, ISSN 0039-128X, https://doi.org/10.1016/j.steroids.2023.109219
18. Šestić, I.L.; Ajduković, J.J.; Marinović, M.A.; Petri, E.T.; Savić, M.P. In Silico ADMET Analysis of the A-, B- and D-Modified Androstane Derivatives with Potential Anticancer Effects. *Steroids* **2023**, *189*, pp. 109147, ISSN 0039-128X, https://doi.org/10.1016/j.steroids.2022.109147
19. Lorca, M.; Cabezas, D.; Araque, I.; Terán, A.; Hernández, S.; Mellado, M.; Espinoza, L.; Mella, J. Cancer and Brassinosteroids: Mechanisms of Action, SAR and Future Perspectives. *Steroids* **2023**, *190*, pp. 109153, ISSN 0039-128X, https://doi.org/10.1016/j.steroids.2022.109153
20. Aslam, M.; Augustine, S.; Mathew, A.A.; Kanthlal, S.K.; Panonummal, R. Apoptosis Promoting Activity of Selected Plant Steroid in MRMT-1 Breast Cancer Cell Line by Modulating Mitochondrial Permeation Pathway. *Steroids* **2023**, *190*, pp. 109151, ISSN 0039-128X, https://doi.org/10.1016/j.steroids.2022.109151
21. Tantawy, M.A.; Shalby, A.B.; Barnawi, I.O.; Kattan, S.W.; Rabou, A.A.A.; Elmegeed, G.A. Anti-Cancer Activity, and Molecular Docking of Novel Hybrid Heterocyclic Steroids Revealed Promising Anti-Hepatocellular Carcinoma Agent: Implication of Cyclin Dependent Kinase-2 Pathway. *Steroids* **2023**, *193*, pp. 109187, ISSN 0039-128X, https://doi.org/10.1016/j.steroids.2023.109187
22. Huang, Y.M.; Cheng, Y.; Peng, Z.N.; Pang, L.P.; Li, J.Y.; Xiao, J.A.; Zhang, Y.F.; Cui, J.G. Synthesis and Antitumor Activity of Some Cholesterol-Based Selenocyanate Compounds. *Steroids* **2023**, *194*, pp. 109217, ISSN 0039-128X, https://doi.org/10.1016/j.steroids.2023.109217
23. Agarwal, D.S.; Sakhuja, R.; Beteck, R.M.; Legoabe, L.J. Steroid-Triazole Conjugates: A Brief Overview of Synthesis and their Application as Anticancer Agents. *Steroids* **2023**, *197*, pp. 109258, ISSN 0039-128X, https://doi.org/10.1016/j.steroids.2023.109258
24. Cooper, R.; Nicola, G. Natural Products Chemistry: Sources, Separations, and Structures. CRC Press Taylor & Francis Group: Broken Sound Parkway, New York, **2015**; pp. 111-124, https://doi.org/
25. Newman, M.S.; Mayfield, B.P.; Saltiel, D.; Stanczyk, F.Z. Assessing Estrogen Exposure from Transdermal Estradiol Patch Therapy Using a Dried Urine Collection and a GC–MS/MS Assay. *Steroids* **2023**, *189*, pp. 109149, ISSN 0039-128X, https://doi.org/10.1016/j.steroids.2022.109149
26. Abtin, S.; Ghasemi, R.; Manaheji, H. Progesterone Modulates the Expression of Spinal Ephrin-B2 After Peripheral Nerve Injury: New Insights into Progesterone Mechanisms. *Steroids* **2023**, *190*, pp. 109155, ISSN 0039-128X, https://doi.org/10.1016/j.steroids.2022.109155
27. Liu, H.; Huan, C.; Nie, L.; Gu, H.; Sun, J.; Suo, X.; Liu, D.; Liu, J.; Wang, M.; Song, Y.; Mao, Z.; Wang, C.; Huo, W. The Association of Cortisol/Testosterone Ratio and Sleep Quality with Coronary Heart Disease: A Case-Control Study in Chinese Rural Population. *Steroids* **2023**, *193*, pp. 109197, ISSN 0039-128X, https://doi.org/10.1016/j.steroids.2023.109197
28. Harlim, T. Content of Marine Algae Steroids Around the Coast of Indonesia. Dissertation. ITB, Bandung, Indonesia, **July 15**, **1982**.
29. Jalalvand, A.R.. Chemometrics-Assisted Electrochemical Biosensing of Cholesterol as the Sole Precursor of Steroids by a Novel Electrochemical Biosensor. *Steroids* **2023**, *190*, pp. 109159, ISSN 0039-128X, https://doi.org/10.1016/j.steroids.2022.109159
30. Jin, Y.X.; Chi, M.J.; Wei, W.K.; Zhao, Y.Q.; Wang, G.K.; Feng, T. Tricholosterols A–D, Four New Ergosterol Derivatives from the Mushroom Tricholoma Terreum. *Steroids* **2023**, *191*, pp. 109157, ISSN 0039-128X, https://doi.org/10.1016/j.steroids.2022.109157
31. Hosoda, K.; Wanibuchi, K.; Amgalanbaatar, A.; Shoji, M.; Hayashi, S.; Shimomura, H. A Novel Role of Catalase in Cholesterol Uptake of Helicobacter Pylori. *Steroids* **2023**, *191*, pp. 109158, ISSN 0039-128X, https://doi.org/10.1016/j.steroids.2022.109158

32. Zhao, H.; Zhong, Z.; Chen, M.; Sun, B.; Wang, J.; Jin, C. Investigation on the Synthesis of 24-(R)-Hydroxycholesterol. *Steroids* **2023**, *195*, pp. 109227, ISSN 0039-128X, https://doi.org/10.1016/j.steroids.2023.109227
33. Mironov, M.E.; Rybalova, T.V.; Pokrovskii, M.A.; Emaminia, F.; Gandalipov, E.R.; Pokrovskii, A.G.; Shults, E.E. Synthesis of Fully Functionalized Spirostanic 1,2,3-Triazoles by the Three Component Reaction of Diosgenin Azides with Acetophenones and Aryl Aldehydes and Their Biological Evaluation as Antiproliferative Agents. *Steroids* **2023**, *190*, pp., 109133, ISSN 0039-128X, https://doi.org/10.1016/j.steroids.2022.109133
34. Hadisuwoyo, M. Rapid Method of Extraction and Purification of Marine Algal Sterols with a Three-Component Solvent System. Thesis. Hasanuddin University, Ujung Pandang, Indonesia, **May 21**, **1995**.
35. Dali, N. Isolation and Identification of Steroids in the Sea Urchin (*Diadema Setosum* Leske) Gonads. Thesis. Hasanuddin University, Ujung Pandang, Indonesia, **April 17**, **1997**.
36. Lambert, J.B.; Gronert, S.; Shurvell, H.F.; Lightner, D.A. Organic Structural Spectroscopy; Pearson Prentice Hall: New York, USA, **2011**, pp. 342.
37. Kemp, W. Organic Spectroscopy; MacMillan Education Ltd.: London, Inggris, **1991**, pp. 58, https://doi.org/10.1007/978-1-349-15203-2
38. Sastrohamidjojo, H. Nuclear Magnetic Resonance Spectroscopy; Liberty: Yogyakarta, Indonesia, **1994**, pp. 68.
39. Folkers, K. The Impact of Natural Product Chemistry on Medicine. *Pure and Applied Chemistry* **1967**, *14(1)*, pp. 1-17, https://doi.org/
40. Talapatra, S.K.; Talapatra, B. Chemistry of Plant Natural Products: Stereochemistry, Conformation, Synthesis, Biology, and Medicine; Springer-Verlag: Heidelberg, New York, **2015**, pp. 553-584, ISBN 978-3-642-45409-7 ISBN 978-3-642-45410-3 (eBook), https://doi.org/10.1007/978-3-642-45410-3
41. Brahmachari, G. Bioactive Natural Products Chemistry and Biology; Wiley-VCH Verlag GmbH & Co.: Weinheim, Germany, **2015**; pp. 473-490, ISBN: 978-3-527-68440-3 (eBook).